JOURNAL OF MATERIALS SCIENCE 28 (1993) 6185–6189

Mechanical properties of γ-aluminium oxynitride

H. X. WILLEMS, P. F. VAN HAL, G. DE WITH*, R. METSELAAR
Centre for Technical Ceramics, Eindhoven University of Technology, P.O. Box 595, 5600 AN Eindhoven, The Netherlands, and also Philips Research Laboratories, P.O. Box 80 000, 5600 JA Eindhoven, The Netherlands

Mechanical properties have been measured of three compositionally different types of γ-aluminium oxynitride (Alon). The compositions corresponded to 67.5, 73 and 77.5 mol% Al_2O_3. To characterize the Alons, lattice parameters, densities, grain sizes and optical properties were measured. The measurements for the mechanical properties comprise hardness at various indentation loads, elastic properties, fracture strength and fracture toughness (at room temperature and at 600 °C).

1. Introduction

The mechanical properties of γ-aluminium oxynitride (Alon) reported in the literature are, in most cases, singular measurements of one or two properties on one or two types of (sometimes poorly characterized) Alon. In this paper a number of properties measured on three well-characterized compositions of Alon are presented. All measurements were performed on Alons with compositions of 67.5, 73 and 77.5 mol% Al_2O_3 and thus cover almost the entire Alon homogeneity region at 1850 °C [1]. The measurements comprise hardness at various indentation loads, elastic properties, fracture strength (at room temperature and at 600 °C) and fracture toughness (also at those two temperatures). The wear properties of Alons with the same compositions in Alon/Y-TZP systems are discussed by Van den Berg *et al.* [2].

The details of the production of the Alons used in this study are reported elsewhere [3]. Three varieties of Alon were made (which were different with regard to their Al_2O_3 content) and in this paper, the Alon composition with 67.5 mol% Al_2O_3 is denoted "L" (for left), whereas Alons with 73 and 77.5 mol% Al_2O_3 are denoted "M" (middle) and "R" (right), respectively.

2. Characterization

The microstructures of the Alons were examined with optical microscopy (OM), scanning electron microscopy (SEM) and transmission electron microscopy (TEM). With TEM, grain boundaries were checked for secondary phases: no grain-boundary phases were observed and boundaries appeared to be smooth and clean. Grain sizes were determined from micrographs (OM and SEM) of polished and thermally etched samples using the linear intercept method, counting about 50 grains on the optical micrographs and 30 grains on the scanning electron micrographs. Thermal etching was performed at 1590 °C in 1 bar of flowing nitrogen for 10 min. The notation a ($\pm$ b) is used, in which *a* denotes the mean value and *b* the sample standard deviation.

Lattice parameters of the Alons were determined with X-ray diffraction. The lattice parameters were 0.7950, 0.7942 and 0.7936 nm ($\pm$ 0.0001 nm) for L, M and R, respectively. Densities were determined with the Archimedes method described by Prokic [4] and values of 3.683, 3.674 and 3.651 g cm^{-3} ($\pm$ 0.002 g cm^{-3}) were found for L, M and R. If these densities are related to the theoretical densities, we find 99.7% for L, 99.7% for M and 99.2% for R ($\pm$ 0.1%). The porosity was also determined with a grid count on micrographs of polished and thermally etched samples, counting six frames of approximately 400 points each. This yielded porosities of 0.56%, 0.55% and 0.83% ($\pm$ 0.3%) for L, M and R, respectively. Within their accuracy, the porosity measurements yield the same results as the density measurements.

A representative optical micrograph (M-type Alon) is shown in Fig. 1. The mean grain size determined from optical micrographs was 25.9 ($\pm$ 6.5) μm for L, 26.9 ($\pm$ 3.2) μm for M and 40.2 ($\pm$ 7.0) μm for R. From scanning electron micrographs, grain sizes of 31.8 ($\pm$ 5.1) μm for L, 40.6 ($\pm$ 13.3) μm for M and 53.0 ($\pm$ 10.1) μm for R were found. There is a reasonable agreement between the grain sizes obtained from the optical micrographs and the grain sizes obtained from the scanning electron micrographs.

The optical properties of the Alons were measured on samples that were polished with 1 μm diamond paste on both sides. For the infrared frequency region, the spectrum was measured between 400 and 4000 cm^{-1} with a double-beam IR spectrophotometer (Hitachi 270-30). For measurements in the visible frequency region, the same method was used with a double-beam UV/VIS spectrophotometer (Hitachi 150-20). The measured range of wavelengths was 200–900 nm. The aperture was about 1 mrad.

The Alons examined in this study are colourless or slightly white in colour (due to the residual porosity). A typical in-line infrared spectrum of translucent Alon (L) is shown in Fig. 2. Maximum transmission was observed at a wave number of about 2350 cm^{-1}

0022–2461

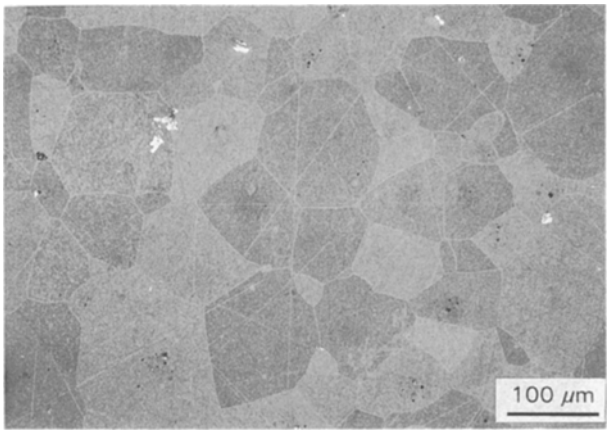

Figure 1 Optical micrograph of Alon with a composition of 73 mol% Al_2O_3.

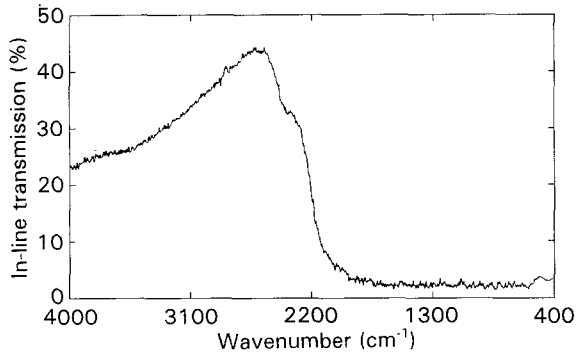

Figure 2 IR transmittance spectrum of Alon with a composition of 73 mol% Al_2O_3.

(wavelength $\approx$ 4.3 μm). The VIS/UV spectrum showed a transmission of approximately 4% over the complete range down to the UV cut-off. As can be seen from these spectra, the material is not completely dense and, as a result, a large part of the light is scattered and low in-line transmittances were measured. Results of the optical measurements are summarized in Table I.

The optical properties of these translucent Alons in terms of in-line transmission are not very impressive compared to the results reported in other papers, which report transmittances of about 80% at an aperture of 1 mrad [5, 6]. This could be caused by the fact that the sintering time for these Alons is shorter than the sintering time of the reaction sintering processes described in the literature. As a consequence, the grain size of this material is lower than the grain size of the materials described in the literature and because the grain boundaries have moved through a smaller fraction of the material, fewer pores have been removed by "grain-boundary sweeping".

3. Experimental procedure

Hardness was measured with indentation, using a Leitz hardness tester (type Miniload 2) with a Vickers diamond indentor. Indentations were made on surfaces that were polished with 1 μm diamond paste. Loads of 4.91, 9.81 and 19.62 N were applied.

TABLE I Optical properties of Alon. The transmission is not corrected for reflection

Composition	Thickness (mm)	I_{max}/I_0 in-line (%)	UV cut-off (nm)	IR cut-off (nm)
L	1.07 ± (0.03)	35	230	7150
M	0.70 ± (0.10)	40	220	7150
R	0.76 ± (0.09)	50	218	7700

The hardness was calculated from:

$$\sigma_f = \frac{1.854F}{d^2} \quad (1)$$

in which F is the applied force and d is the diagonal of the indentation. The reported results are mean values obtained from 15–20 indentations.

The elastic properties were determined with the pulse-echo technique. Three specimens of each composition were tested. The longitudinal wave velocity, v_l, and the shear wave velocity, v_t, were measured at 20 and 5 MHz, respectively. From these velocities Poisson's ratio, ν, and Young's modulus, E, can be calculated according to Equations 2 and 3, in which ρ is the density of the material [7]

$$\nu = \frac{1}{2} - \frac{v_t^2}{2(v_l^2 - v_t^2)} \quad (2)$$

$$E = 2\rho v_t^2(1 + \nu) \quad (3)$$

The fracture strength was measured by three-point bending (3PB) at room temperature and at 600 °C. The latter temperature was chosen in order to have no interference by oxidation [8]. Specimens were bars $15 \times 3 \times 1$ mm^3 in size, with a surface roughness of 0.5 μm. Experiments were done on an Erichsen testing machine (type 476) with a crosshead speed of 5 mm min^{-1}. For each result, ten specimens were used. The fracture strength was determined using Equation 4 in which σ_f is the fracture strength, F is the fracture force, S is the span length (12 or 10.2 mm in this case), B is the width (1 mm) and W is the height (3 mm) of the bar.

$$\sigma_f = \frac{3FS}{2BW^2} - 0.266\frac{F}{BW} \quad (4)$$

The second part of this equation is the Seewald–Von Karman correction [9, 10] which accounts for the wedging effect in three-point bending. This wedging effect perturbs the linear stress profile and is a result of the concentrated contact force from the loading roller acting upon the bend bar. For the configuration used here the correction is about 5%.

The Weibull modulus, m, can be calculated from

$$\ln\left[\ln\left(\frac{1}{1 - P_f}\right)\right] = m\ln(\sigma) + C \quad (5)$$

in which C is a constant [11]. The failure probability, P_i, is estimated from $P_i = (i - 0.5)/n$, in which i is the order number of the tested specimen and n is the total number of specimens tested ($n = 10$ in this case).

A weighted linear least-squares fit procedure was used with weights $w_i = (1 - P_i)\ln(1 - P_i)$.

For the room-temperature measurements, a stainless steel bend jig with a span length of 12 mm was used. The measurements were performed in flowing nitrogen with a dew point lower than $-35\,^{\circ}C$. The measurements at 600 °C were performed in air in an aluminium oxide bend jig with a span length of 10.2 mm.

The fracture toughness was measured with the single-edge notched beam technique (SENB). For these measurements the same kind of specimens as for the fracture toughness measurements were used; this time, however, a small groove was machined in the $15 \times 1\ mm^2$ face of the specimens. The depth of the groove was approximately 400 μm, the width approximately 100 μm. The experimental circumstances were the same as mentioned for the fracture strength measurements. No precracking was done. For each result five specimens were tested. The fracture toughness, K_{Ic}, was calculated from [12]

$$K_{Ic} = Y\frac{3FS}{2BW^2}a^{1/2} \quad (6)$$

in which a is the depth of the groove and Y is a compliance function given by

$$Y = 1.93 - 3.07\left(\frac{a}{W}\right) + 14.53\left(\frac{a}{W}\right)^2 - 25.11\left(\frac{a}{W}\right)^3 + 25.80\left(\frac{a}{W}\right)^4 \quad (7)$$

It has been shown [13], that experiments that use specimens of this size yield reliable values for the fracture toughness, while making efficient use of the available material.

4. Results

The hardness shows a dependency on the applied load and a slight dependence on the composition of the sample. Results are summarized in Table II. At low loads the impression of the diamond is rather small and consequently measuring the dimensions of the indentation is not easy. At high loads sometimes cracking occurs in the material. In Fig. 3 the results are shown to give an impression of the dependence of the hardness on the applied load and the type of Alon. The data points of the M-type Alon have been shifted horizontally to obtain a less cluttered figure.

The results from the measurements of the elastic properties are summarized in Table III. The elastic properties are dependent on the composition of the Alon, but the differences are relatively small. The obtained values together with data from literature [14] are shown in Fig. 4a and b. As can be seen from this figure, our data do agree with the data from the literature.

Results from the fracture strength and the fracture toughness measurements are summarized in Tables IV and V. No dependency of σ_f or K_{Ic} on the composition of the specimens was found. With SEM observations on the broken surfaces it was determined that fracture is mainly transgranular.

TABLE II Hardness of Alons measured at three different loads. The reported results are the values of the mean and the sample standard deviation obtained from 15–20 measurements

Composition	Hardness (GPa)		
	4.905 N	9.81 N	19.61 N
L	19.93 (± 1.65)	17.70 (± 0.67)	16.93 (± 0.56)
M	17.94 (± 0.71)	17.67 (± 1.13)	16.11 (± 0.76)
R	16.87 (± 1.17)	16.07 (± 0.70)	15.12 (± 0.49)

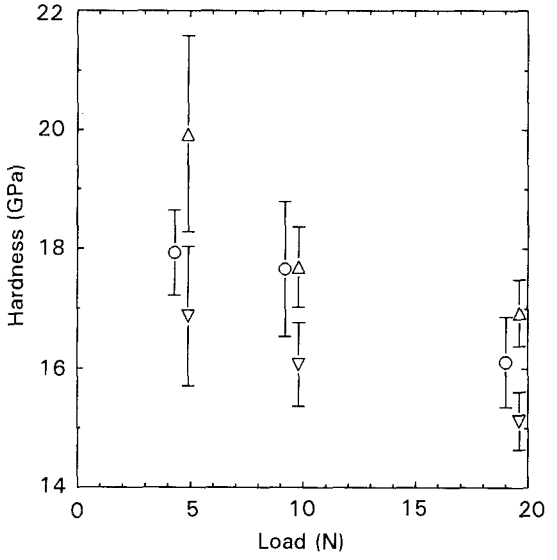

Figure 3 The dependence of the hardness of Alon on the applied load and the composition. (△) L, (○) M, (▽) R. The data points of the M composition have been shifted horizontally to obtain a less cluttered figure.

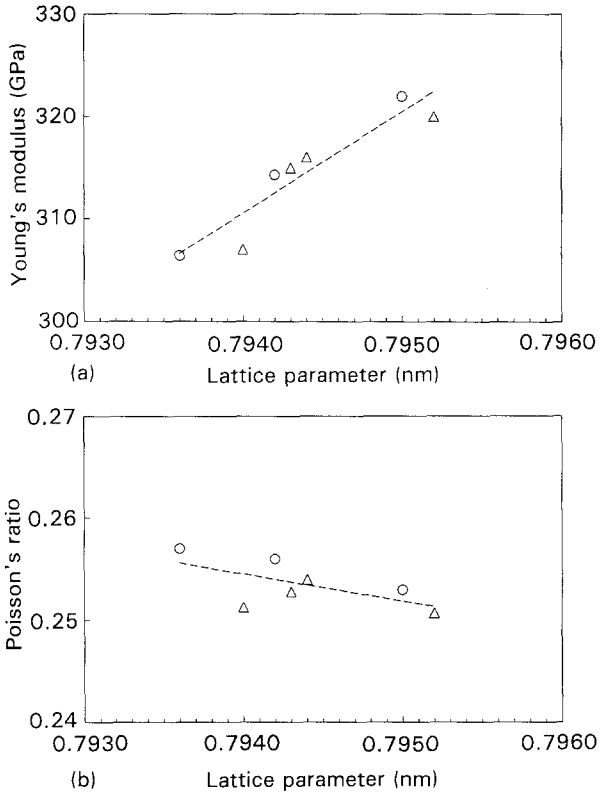

Figure 4 Elastic properties of Alon as a function of the lattice parameter. (○) Results for this investigation, (△) literature data from Graham *et al.* [14]; (a) Young's modulus, (b) Poisson's ratio.

TABLE III Elastic properties of Alon (three specimens)

Property		Composition (mol% Al_2O_3)		
		L (67.5)	M (73)	R (77.5)
v_l	(km s^{-1})	10.270 (± 0.004)	10.186 (± 0.004)	10.100 (± 0.004)
v_t	(km s^{-1})	5.907 (± 0.003)	5.837 (± 0.003)	5.779 (± 0.003)
Young's modulus	(GPa)	322.0 (± 0.5)	314.3 (± 0.5)	306.4 (± 0.5)
Poisson's ratio		0.253 (± 0.002)	0.256 (± 0.002)	0.257 (± 0.002)

5. Discussion

The three types of Alon tested here do show a very similar behaviour. With respect to fracture strength and fracture toughness, no differences between the various Alon types were observed, due to the rather large statistical errors in the determination of these quantities. The quantities with a smaller variance do show a slight dependence on the composition.

The obtained hardness values are slightly higher than the values reported in literature [5, 6, 15]. This is probably caused by the lower porosity in our specimens compared to the porosity of the specimens that were used for the hardness measurements in the literature.

The fracture strength measurements yield a relatively high value for σ_f compared to the values from the literature (see Table VI). The value obtained here will be relatively high because the actual volume tested in our experiments is rather small: this is because the specimens are small and three-point bending is used. The relation between the volume of the test bar and the strength obtained is given by Equation 8 in which $\bar{\sigma}_i$ is the mean fracture strength, V_i is the volume of the test bar and m is the Weibull modulus of the material (≈ 8).

$$\frac{\bar{\sigma}_2}{\bar{\sigma}_1} = \left(\frac{V_1}{V_2}\right)^{1/m} \tag{8}$$

The highest fracture strength reported in the literature for three-point bending and recalculated for our size

TABLE IV Fracture strength (ten specimens) and Weibull moduli of Alon

Composition	Fracture strength (MPa)		Weibull modulus	
	$T = 20\,°C$	$T = 600\,°C$	$T = 20\,°C$	$T = 600\,°C$
L	455 (± 55)	314 (± 38)	7.9	12.5
M	500 (± 51)	294 (± 26)	9.8	10.0
R	494 (± 72)	289 (± 22)	7.3	12.8

TABLE V Fracture toughness of Alon (five specimens)

Composition	Fracture toughness (MPa $m^{1/2}$)	
	$T = 20\,°C$	$T = 600\,°C$
L	2.79 (± 0.17)	1.87 (± 0.22)
M	2.66 (± 0.30)	2.07 (± 0.11)
R	2.86 (± 0.42)	1.87 (± 0.16)

TABLE VI Literature values on the strength of Alon

σ_f (MPa)	Method	Temperature (°C)	Grain size (μm)	Fabrication	Density (g cm^{-3} or %)	Remarks	Reference
50–300	3PB	20	–	Hot pressed	> 98%	Not pure	[17]
306	4PB	20	25	Reaction sintered	3.639		[18]
267		1000					[19]
190		1200					
256	4PB	20	100	Reaction sintered	3.648		[18]
307 (± 26)	4PB	20	100	Sintered	3.65	95%–98% Alon	[16]
305 (± 27)					3.61		
262 (± 15)	4PB	20	100	Sintered		95%–98% Alon	[16]
257 (± 30)	4PB	20	25	Reaction sintered		> 98% Alon	[16]
280			25			> 98% Alon	
200–300		20	200	Reaction sintered	> 99.6%		[5]
300 (± 34)	4PB	20	145				[6]
279		600					
299 (± 96)	3PB			Reaction sintered		0% Y_2O_3	[15]
340 (± 126)						0.8% Y_2O_3	
278 (± 57)						1.66% Y_2O_3	
200 (± 10)	3PB	20	200–300	Hot pressed			[20]
100 (± 50)		1000					
140 (± 20)		1200					

of specimen is about 320 MPa [16]. For the majority of the tests in the literature, four-point bending was used to measure the fracture strength. The relation with strengths measured with three-point bending is given by [11]

$$\frac{\overline{\sigma_{3PB}}}{\overline{\sigma_{4PB}}} = \left(\frac{V_{4PB}}{V_{3PB}}\right)^{1/m} \left(\frac{m+2}{2}\right)^{1/m} \quad (9)$$

The maximum 4PB strengths reported in the literature are 300 MPa and these were measured on specimens with test volumes $2 \times 10 \times 40$ and $2.2 \times 2.8 \times 30$ mm^3 [6, 15] using transparent samples with grain sizes of 100–145 μm. If these values are recalculated for 3PB testing and our specimen size, then we obtain values of 522 and 450 MPa.

On the other hand, the measurements reported in the literature make no use of wedging corrections and therefore our values have to be increased with approximately 5% to make a comparison possible. The fracture strength found in this study with translucent samples is as good as or better than the strength values obtained with transparent material. This could be due to the lower grain size of our samples.

The Weibull modulus is larger than that determined by Chen *et al.* [16]: they found $m \approx 3$ at room temperature while we found $m \approx 8$ at room temperature and $m \approx 12$ at 600 °C. Chen *et al.* used $P_i = i/(n+1)$ instead of $P_i = (i - 0.5)/n$ and this yields a somewhat lower value for the Weibull modulus. However, this can only partly explain the difference in the values obtained and therefore their materials must have been more inhomogeneous than ours.

The K_{Ic} values obtained here are slightly higher than the values from the literature [6, 15]. This could be due to the low porosity of our samples compared to the samples that were used for the determination of the fracture toughness in the literature.

The fracture strength and the fracture toughness at 600 °C are significantly lower than at room temperature. The decrease in fracture strength is as large as the decrease in fracture toughness, which indicates no change in failure mechanism.

6. Conclusion

Several mechanical and optical properties of three types of Alon have been measured. The various types of Alon have properties that are very much alike. The fracture strength and the fracture toughness are approximately equal for the three Alons. A slight dependence on the composition is observed when the experimental variance is not too large. This dependence is probably partly obscured by the variation in grain sizes between the different materials.

If the amount of Al_2O_3 increases, the hardness, the Young's modulus and the UV cut-off decrease, while the grain size, the value of the Poisson's ratio, the in-line transmission and the IR cut-off increase. The grain sizes are, on average, smaller than those reported in the literature. The in-line transmission of Alons produced in this study is lower than that of Alons in literature while the hardness, the fracture strength and the fracture toughness values are higher than those reported in the literature.

Acknowledgement

This research has been partly sponsored by the Commission for the Innovative Research Program Technical Ceramics (IOP-TK) of the Ministry of Economic Affairs in the Netherlands (IOP-TK research grant 88.A022).

References

1. H. X. WILLEMS, M. M. R. M. HENDRIX, G. DE WITH and R. METSELAAR, *J. Eur. Ceram. Soc.* **10** (1992) 339.
2. P. H. J. VAN DEN BERG, H. X. WILLEMS and G. DE WITH, *J. Mater. Sci.* accepted.
3. H. X. WILLEMS, M. M. R. M. HENDRIX, G. DE WITH and R. METSELAAR, in "Proceedings of the 2nd Conference of the European Ceramic Society", Augsburg, Germany, 10–14 September, 1991 (in press).
4. D. PROKIC, *J. Phys. D Appl. Phys.* **7** (1974) 1873.
5. G. ADO, M. BILLY, P. GUILLO and P. LEFORT, *Ind. Ceram.* **792** (1985) 173.
6. T. M. HARTNETT and R. L. GENTILMAN, *Proc. SPIE Int. Soc. Opt. Eng.* **505** (1984) 15.
7. H. F. POLLARD, "Sound waves in solids" (Pion, London, 1977).
8. P. GOURSAT, P. GOEURIOT and M. BILLY, *Mater. Chem.* **1** (1976) 131.
9. S. P. TIMOSHENKO and J. N. GOODIER, "Theory of Elasticity", 3rd Edn, (McGraw-Hill, London, 1970).
10. G. DIAZ and P. KITTL, *Res. Mech.* **24** (1988) 209.
11. W. E. C. CREYKE, I. E. J. SAINSBURY and R. MORRELL, "Design with non-ductile materials" (Applied Science, London, 1982).
12. W. F. BROWN and J. E. STRAWLEY, "Plane strain crack toughness testing of high strength materials", ASTM-STP-410 (American Society for Testing Materials, Philadelphia, PA, 1967).
13. G. DE WITH and N. HATTU, *J. Mater. Sci.* **16** (1981) 1702.
14. E. K. GRAHAM, W. C. HUNLY, J. W. McCAULEY and N. D. CORBIN, *J. Am. Ceram. Soc.* **71** (1988) 807.
15. G. D. QUINN, N. D. CORBIN and J. W. McCAULEY, *ibid.* **63** (1984) 723.
16. C.-F. CHEN, E. SAVRUN and A. F. RAMIREZ, in "Ceramics today – tomorrow's ceramics", edited by P. Vincenzini (Elsevier, Amsterdam, 1990) p. 1295.
17. R. KIEFFER, W. WRUSS and B. WILLER, *Rev. Int. Hautes Temp. Refrac.* **13** (1976) 97.
18. N. D. CORBIN and J. W. McCAULEY, *Proc. SPIE Int. Soc. Opt. Eng.* **297** (1981) 19.
19. T. M. HARTNETT, E. A. MAGUIRE, R. L. GENTILMAN, N. D. CORBIN and J. W. McCAULEY, *Ceram. Eng. Sci. Proc.* **3** (1982) 67.
20. P. LEFORT, P. ADO and M. BILLY, *Sci. Ceram.* **14** (1988) 697.

Received 25 November 1992
and accepted 2 April 1993